Published in final edited form as:
Angew Chem Int Ed Engl. 2014 July 28; 53(31): 8104–8107. doi:10.1002/anie.201402216.

Pericellular Hydrogel/Nanonets Inhibit Cancer Cells

Dr. Yi Kuang,
Department of Chemistry, Brandeis University, 415 South St, Waltham, MA 02454, USA, Fax: (+) 1-781-736-2516, Homepage: http://people.brandeis.edu/~bxu

Mr. Junfeng Shi,
Department of Chemistry, Brandeis University, 415 South St, Waltham, MA 02454, USA, Fax: (+) 1-781-736-2516, Homepage: http://people.brandeis.edu/~bxu

Ms. Jie Li,
Department of Chemistry, Brandeis University, 415 South St, Waltham, MA 02454, USA, Fax: (+) 1-781-736-2516, Homepage: http://people.brandeis.edu/~bxu

Ms. Dan Yuan,
Department of Chemistry, Brandeis University, 415 South St, Waltham, MA 02454, USA, Fax: (+) 1-781-736-2516, Homepage: http://people.brandeis.edu/~bxu

Mr. Kyle A. Alberti,
Department of Biomedical Engineering, Tufts University, 419 Boston Ave, Medford, MA 02155, USA

Prof. Qiaobing Xu, and
Department of Biomedical Engineering, Tufts University, 419 Boston Ave, Medford, MA 02155, USA

Prof. Dr. Bing Xu
Department of Chemistry, Brandeis University, 415 South St, Waltham, MA 02454, USA, Fax: (+) 1-781-736-2516, Homepage: http://people.brandeis.edu/~bxu

Bing Xu: bxu@brandeis.edu

Abstract

Fibrils formed by proteins are vital components for cells. However, selective formation of xenogenous nanofibrils of small molecules on mammalian cells has yet to be observed. Here we report an unexpected observation of hydrogel/nanonets of a small D-peptide derivative in pericellular space. Surface and secretory phosphatases dephosphorylate a precursor of a hydrogelator to trigger the self-assembly of the hydrogelator and to result in pericellular hydrogel/nanonets selectively around the cancer cells that overexpress phosphatases. Cell based assays confirm that the pericellular hydrogel/nanonets block cellular mass exchange to induce apoptosis of cancer cells, including multidrug-resistance (MDR) cancer cells, MES-SA/Dx5. Pericellular hydrogel/nanonets of small molecules to exhibit distinct functions illustrates a fundamentally new

Correspondence to: Bing Xu, bxu@brandeis.edu.

Supporting information for this article is available on the WWW under http://www.angewandte.org or from the author.

way to engineer molecular assemblies spatiotemporally in cellular microenvironment for inhibiting cancer cell growth and even metastasis.

Keywords

pericellular; hydrogel; nanofibrils; cancer; inhibition

Besides serving as important internal components (e.g., cytoskeletons) of cells, fibrils outside the cells also bear significant functions. For example, fibrils formed by polysaccharides and fibrous proteins, such as fibronectin, collagens, and laminins,[1] afford networks that withhold extracellular fluid, and the resulting extracellular matrix maintains multicellular structures and mediates celL-cell communication.[2] A recent study demonstrated that human α-defensin 6 (HD6) self-assembles in contact with bacteria surface protein to form nanonets that entrap the bacteria and block their translocation.[3] The various functionalities of extracellular fibrils and networks formed by biomolecules suggest that it is feasible to build xenogenous fibrils extracellularly (e.g., in the pericellular space) as a new approach for regulating the interaction of cell with its microenvironment,[4] thus controlling the fate of cells.

Like self-assembling peptides and proteins, certain small organic molecules self-assemble [5] in water to afford nanofibrils as matrices of hydrogels[6] (e.g., in response to biostimuli such as enzymes[7]). Interestingly, a vancomycin-pyrene conjugate, which self-assembles in water to form nanofibrils,[8] exhibits two orders of magnitude enhanced antibacterial activity against vancomycin resistant enterococci (VRE), plausibly through self-assembled multivalent vancomycin binding the receptors on bacterial cell wall.[9] However, the observation of xenogenous nanofibrils on mammalian cells has yet to be reported. During our research of enzyme catalyzed self-assembly of D-peptide derivatives,[10] the self-assembly of a small D-peptide derivative, surprisingly, forms pericellular hydrogel/nanonets. Here, we report the observation, the origin of formation, and a potential application (i.e., inhibiting cancer cells) of the pericellular hydrogel/nanonets.

As illustrated in Fig. 1a, our results show that (i) surface and secretory phosphatases[11] from cells catalytically dephosphorylate a small D-peptide derivative (e.g., D-**1**) to form a hydrogelator (e.g., D-**2**); (ii) the accumulation of the hydrogelator results in a network of nanofibrils as the scaffold of a hydrogel in the pericellular space; (iii) the pericellular hydrogel/nanonets entrap secretory proteins, block cellular uptake, thus decreasing cell migration, preventing cell adhesion, and induce cell apopotosis; (iv) most importantly, due to the overexpression of surface and secretory phosphatases by cancer cells,[12] the pericellular nanonets selectively form on the cancer cells (e.g., HeLa, MES-SA, and MES-SA/Dx5). As an unexpected example of enzyme-instructed self-assembly[7c] in pericellular space, this work illustrates a new way that controls the fate of different types of cells according to the expression and location of enzymes that regulate the spatiotemporal profiles of molecular nanofibrils.

Being synthesized according to the reported procedure[13] and consisting of a naphthalene capped tripeptide, D-Phe-D-Phe-D-Tyr, molecule D-**1** differs with D-**2** only in that the D-

Tyr is phosphorylated (Fig. 1b). Like a previous work on enzyme-instructed self-assembly of D-peptides,[10b] alkaline phosphatase (ALP) catalyzes the dephosphorylation of the precursor (D-**1**; 0.20 wt%/2.77 mM) to form the hydrogelator (D-**2**; 0.18 wt%/2.77 mM), which self-assembles in water to form nanofibrils and to result in a hydrogel in PBS buffer. However, an unexpected phenomenon occurred when incubating HeLa cells with D-**1**. As shown in Fig. 2a, the incubation of a confluent layer of HeLa cells (in a 35 mm Petri dish) in complete culture medium (1 mL) containing D-**1** (560 μM) results in a layer of hydrogel-like soft materials on the cells after 2 h of incubation at 37 °C. While reducing the concentration of D-**1** to 280 μM still causes hydrogelation on cells (Fig. 2b), little such hydrogel occurs on the HeLa cells treated by D-**1** at 140 μM (Fig. 2c). LC-MS analysis reveals that the hydrogel contains D-**2** at about 2.05 mM (table S1), much higher than the concentration used for incubation. This result suggests that the conversion of D-**1** to D-**2** leads to the pericellular accumulation of D-**2** for the hydrogelation on the HeLa cells. In contrast, the incubation of HeLa cells with D-**2** at even 560 μM hardly results in hydrogelation (Fig. 2d), further suggesting that phosphatases catalyzed dephosphorylation of D-**1** results in localized self-assembly of D-**2** in the pericellular space for hydrogelation. This notion agrees with that the phosphatase inhibitors (Pierce™) prevent forming the pericellular hydrogel around the HeLa cells (Fig. S2a).

HeLa cell conditioned medium also dephosphorylates D-**1** to result in hydrogelation. After 48h of incubation, the medium treated by D-**1** at 560 μM completely transforms from a solution to a hydrogel (Fig. S1a, b), and the medium treated by D-**1** at 280 μM also contains clots of hydrogels in the solution. Being similar to the case of HeLa cells, the medium containing D-**1** at 140 μM or D-**2** at 560 μM fails to form a hydrogel (Fig. S1c, d). These results confirm that the secretory phosphatases from the HeLa cells convert D-**1** to D-**2** and contribute to the transition from the solution to the hydrogel. Because of the presence of surface and secretory phosphatases on/near cell membrane, the concentration of phosphatases is high in pericellular space, thus, more D-**2** accumulates and localizes in the pericellular space to self-assemble for hydrogelation. Being directly incubated with the cells at 560 μM (Fig. 2d), D-**2** distributes homogenously in the culture medium (like the case of Fig. S1d), thus it is unable to accumulate on cells to form pericellular hydrogels. Moreover, the incubation of HeLa cells with D-**1** (at 560 μM) and ALP (0.1 U/mL) for 2h hardly results in pericellular hydrogelation (Fig. S2b), suggesting that the gradient of phosphatases is critical for the dynamics of the pericellular accumulation of the hydrogelators (i.e., D-**2**). Although it remains difficult to distinct the contributions from surface and secreted phosphatases, the much faster gelation in the presence of the cells than the cell conditioned medium implies more contribution from the surface phosphatases. We speculate that the major phosphatases for the dephosphorylation of D-**1** are placental alkaline phosphatases (PLAP), which exist in both membrane-bound and secretory forms and exhibit elevated expression in cervical adenocarcinoma cells (HeLa)[14] and uterine sarcoma cells[15] (MES-SA; MES-SA/Dx5).

Scanning electron microscopy (SEM) reveals that the surface of the HeLa cells incubated with D-**1** differs from that of the untreated HeLa cells. Because the organic solvent (e.g., alcohol or acetone) used in cell fixation and the repeated washing destroy the

supramolecular hydrogels, we had to freeze-dry the cells grown on a glass slide for preserving the structure of the nanofibrils in the hydrogels. As shown in Fig. 2e, while the untreated HeLa cells exhibit a smooth surface, the cells treated with D-**1** at 560 μM show a completely different morphology of porous structures cover the surfaces of the cells (i.e. nanonets). Additionally, the cells treated with D-**1** at 280 μM display fiber-like structures attached closely to the cell surface (Fig. S3). These results coincide with the pericellular hydrogelation on HeLa cells treated with D-**1** at 280 and 560 μM. The transmission electron microscope (TEM) image of the pericellular hydrogel on HeLa cells treated by D-**1** at 280 μM reveals that the hydrogel consists of networks of nanofibrils (Fig. 2f) that have diameters about 20 nm (Fig. 2g). That is, the nanofibrils form nanonets. Similar to the nanofibrils of D-**2** formed by the addition of ALP into the solution of D-**1** in PBS buffer (fig. S4), these nanofibrils on the cell surface entangle with each other to form the matrices of the hydrogel. Moreover, TEM shows the rough dark edges on the pericellular nanofibrils (Fig. 2g), indicating that other biomacromolecules likely attach to the nanofibrils.

Congo red and DAPI,[16] a stain for nanofibrils formed by self-assembly[17] and a nucleus dye, respectively, help further visualize the pericellular hydrogel/nanonets on single cells. As shown in Fig. 3a, after incubation with D-**1** at 280 μM for 12 h and the addition of Congo red and DAPI, HeLa cells show obvious red fluorescence that outlines the cell shape, while untreated HeLa cells (i.e., the control) show little red fluorescence. Moreover, DAPI is unable to enter the HeLa cells treated with D-**1** at 280 μM and co-localizes with Congo red, as shown in both the 2-D image and the 3-D stacked image (see video in supplementary materials). This result differs drastically from the staining of the untreated HeLa cells (i.e., DAPI stains the nuclei) and confirms that (i) the hydrogel/nanonets form exclusively in pericellular space and (ii) the pericellular hydrogels/nanonets prevent the diffusion of DAPI into the cells. Since DAPI is a small molecule (M.W. = 277 Da), the block of the cell entry of DAPI suggests that the pericellular hydrogel/nanonets are able to block other molecules (e.g., biomacromolecules) entering cells. The uneven distribution of the Congo red on the surface of the D-**1** treated HeLa cells agrees with the result from SEM, suggesting the inhomogeneous distribution of the hydrogel on the surface of the HeLa cells.

We treated Ect1/E6E7 cells (immortalized normal human cervical epithelial cells, which have same tissue and organ origins as HeLa cells) with the same procedure as that on the HeLa cells. The Ect1/E6E7 cells, after being incubated with D-**1** even at 560 μM for 12 h, hardly display any red fluorescence, which is similar to that of the untreated Ect1/E6E7 cells, and DAPI stains the nuclei of both the treated and the untreated Ect1/E6E7 cells (Fig. 3a). These results agree with that hydrogels hardly form on Ect1/E6E7 cells even for a prolonged incubation time of 48 h (Fig. S5). The difference of hydrogel/nanonets formation by D-**1** on HeLa cells and Ect1/E6E7 cells agrees with that HeLa cells have higher levels phosphatase activities than Ect1/E6E7 cells do (Fig. S6).

To verify whether the pericellular hydrogel/nanonets block secretory proteins/enzymes into the culture medium, we evaluated the amount of phosphatases in the four samples: the blank medium (Blank), medium incubated with untreated HeLa cells (Control), pericellular hydrogel on HeLa cells treated by D-**1** at 560 μM for 12 h (Gel), and the suspension of the medium of HeLa cells treated by D-**1** after removing the hydrogel (Suspension). According

to the result shown in Fig. 3b, the amount of phosphatases accumulated in the Gel is about 27 times higher than that in the Control. Consequently, the amount of phosphatases in the Suspension is significantly lower than that in the Control. These results indicate that the pericellular hydrogel/nanonets capture the secretory proteins/enzymes from the cells, thus blocking them to enter the culture medium. Moreover, we analyzed the protein composition in the four samples by SDS-PAGE and Coomassie staining (Fig. 3c) and found that the Gel lane contains more bands than in the lanes of the Control and the Suspension, suggesting that the pericellular hydrogel/nanonets block diffusion to enrich secretory proteins. In other words, the pericellular hydrogel/nanonets largely block cellular mass exchange between the cells with their environment.

Blocking cellular mass exchange has profound effects on critical cellular activities (e.g., migration, adhesion, and proliferation) of the cancer cells. According to migration assay[18] shown in Fig. S7a, the HeLa cells treated by D-**1** at 280 and 560 μM have gaps larger than that of the untreated HeLa cells (i.e., the control) and those of the HeLa cells treated by D-**1** at 140 μM or D-**2** at 560 μM, confirming that the pericellular hydrogel/nanonets decrease the migration of the HeLa cells. Moreover, as shown by the time progression curve of the cell adhesion (Fig. S7b) of trypsinized HeLa cells,[19] the addition of D-**1** at 560 μM significantly delays the adhesion of HeLa cells (i.e., less than 5% cells reattach to surface after at 4h). The addition of D-**2** at 560 μM, though exhibiting a slight delay of adhesion at the beginning of incubation, hardly hampers cell adhesion (e.g., being similar to that of control, more 80% of cells reattach at 4h). Most importantly, as shown in Fig. 3d, at 280 μM, D-**1** significantly decreases the viability of the HeLa cells to about 10% after 48 h incubation. Moreover, 280 μM of D-**1** also forms pericellular hydrogel/nanonets (Fig. S8) and inhibits the growth of MES-SA and MES-SA/dx5 cells, regardless of the multi-drug resistance of the latter. In contrast, over 60% of the Ect1/E6E7 cells treated with D-**1** at 280 μM for 48 h remain viable. The direct addition of D-**2** at 280 μM hardly inhibits the growth of HeLa cells. These results confirm that the pericellular dephosphorylation of D-**1** leads to the self-assembly of D-**2** on the surface of cancer cells, thus the network of nanofibrils on the cancer cells inhibit the entrapped cells (Fig. S9). We used ELISA to quantify the amount of several key apoptosis signal molecules over time in the HeLa cells incubated with D-**1** at 280 μM (Fig. 3e), and we found that the amount of active Caspase 3 and active PARP increase at 24 and 32 h of incubation, suggesting that the cells undergo mitochondria mediated apoptosis. The apoptosis of the HeLa cells also implies that the toxicity of pericellular hydrogel/nanonets unlikely originates from the perturbation of plasma membrane, which primarily results in necrosis of the cells.[20] Moreover, the removal of the media containing D-**1** (at gradient concentration) after 4 hour incubation restores cell viability (Fig. S12), suggesting little tight ligand-receptor type interaction between D-**2** (or the nanofibrils of D-**2**) with plasma membrane to disrupt the plasma membrane of cells.

One key prerequisite for pericellular hydrogelation is the proteolytic stability of the small molecular precursors and hydrogelators. The incubation of HeLa cells with L-**1** (the L-peptide counterpart of D-**1**; Fig. S10) at 560 μM at 37 °C fails to form pericellular hydrogel/nanofibrils due to the proteolysis of L-**1** in cellular environment (Fig. S11).

In summary, this work demonstrates that molecular nanofibers, formed by enzyme-instructed self-assembly of innocuous monomers, selectively inhibit cancer cells. The rapid formation of the pericellular D-peptide hydrogels contributes to the entrapment of secretory phosphatases in the hydrogel, suggesting a fundamentally new way, which relies on the localization of enzymes, to form supramolecular hydrogels/nanofibrils in a specific cellular location for controlling the fate of cells.[21] In addition, the pericellular hydrogelation also promises a new method that enriches and regulates secretome of cells for understanding and modulating cellular microenvironment.

Supplementary Material

Refer to Web version on PubMed Central for supplementary material.

Acknowledgments

This work was partially supported by NIH(R01CA142746). We acknowledge the help of EM facility in Brandeis University. YK thanks KAA for the help on SEM.

References

1. Persikov AV, Brodsky B. Proc Natl Acad Sci U S A. 2002; 99:1101. [PubMed: 11830649]
2. Mann S. Angew Chem Int Edit. 2008; 47:5306.
3. Chu HT, Pazgier M, Jung G, Nuccio SP, Castillo PA, de Jong MF, Winter MG, Winter SE, Wehkamp J, Shen B, Salzman NH, Underwood MA, Tsolis RM, Young GM, Lu WY, Lehrer RI, Baumler AJ, Bevins CL. Science. 2012; 337:477. [PubMed: 22722251]
4. Iida N, Dzutsev A, Stewart CA, Smith L, Bouladoux N, Weingarten RA, Molina DA, Salcedo R, Back T, Cramer S, Dai RM, Kiu H, Cardone M, Naik S, Patri AK, Wang E, Marincola FM, Frank KM, Belkaid Y, Trinchieri G, Goldszmid RS. Science. 2013; 342:967. [PubMed: 24264989]
5. a) Lehn JM. Science. 2002; 295:2400. [PubMed: 11923524] b) Whitesides GM, Grzybowski B. Science. 2002; 295:2418. [PubMed: 11923529]
6. a) Estroff LA, Hamilton AD. Chem Rev. 2004; 104:1201. [PubMed: 15008620] b) Zhang MM, Xu DH, Yan XZ, Chen JZ, Dong SY, Zheng B, Huang FH. Angew Chem Int Edit. 2012; 51:7011.c) Kiriya D, Ikeda M, Onoe H, Takinoue M, Komatsu H, Shimoyama Y, Hamachi I, Takeuchi S. Angew Chem Int Edit. 2012; 51:1553.d) Tamesue S, Takashima Y, Yamaguchi H, Shinkai S, Harada A. Angew Chem Int Edit. 2010; 49:7461.
7. a) Yang ZM, Gu HW, Fu DG, Gao P, Lam JK, Xu B. Adv Mater. 2004; 16:1440.b) Toledano S, Williams RJ, Jayawarna V, Ulijn RV. J Am Chem Soc. 2006; 128:1070. [PubMed: 16433511] c) Yang Z, Liang G, Xu B. Accounts Chem Res. 2008; 41:315.d) Yuan JP, Wen D, Gaponik N, Eychmuller A. Angew Chem Int Edit. 2013; 52:976.e) Kumar RK, Yu XX, Patil A, Li M, Mann S. Angew Chem Int Edit. 2011; 50:9343.f) Williams RJ, Smith AM, Collins R, Hodson N, Das AK, Ulijn RV. Nat Nanotechnol. 2009; 4:19. [PubMed: 19119277]
8. Xing BG, Yu CW, Chow KH, Ho PL, Fu DG, Xu B. J Am Chem Soc. 2002; 124:14846. [PubMed: 12475316]
9. Xing BG, Ho PL, Yu CW, Chow KH, Gu HW, Xu B. Chem Commun. 2003:2224.
10. a) Li JY, Kuang Y, Gao Y, Du XW, Shi JF, Xu B. J Am Chem Soc. 2013; 135:542. [PubMed: 23136972] b) Li JY, Gao Y, Kuang Y, Shi JF, Du XW, Zhou J, Wang HM, Yang ZM, Xu B. J Am Chem Soc. 2013; 135:9907. [PubMed: 23742714]
11. Wu CC, Hsu CW, Chen CD, Yu CJ, Chang KP, Tai DI, Liu HP, Su WH, Chang YS, Yu JS. Mol Cell Proteomics. 2010; 9:1100. [PubMed: 20124221]
12. Fishman WH, Inglis NR, Green S, Anstiss CL, Gosh NK, Reif Rustigia AE, Krant RMJ, Stolbach LL. Nature. 1968; 219:697. [PubMed: 5691166]
13. Yang Z, Liang G, Ma M, Gao Y, Xu B. Small. 2007; 3:558. [PubMed: 17323399]

14. Elson NA, Cox RP. Biochem Genet. 1969; 3:549. [PubMed: 4983958]
15. Nelson KG, Haskill JS, Sloan S, Siegfried JM, Siegal GP, Walton L, Kaufman DG. Cancer Res. 1987; 47:2814. [PubMed: 3567904]
16. Kapuscinski J. Biotech Histochem. 1995; 70:220. [PubMed: 8580206]
17. Binder WH, Smrzka OW. Angew Chem Int Edit. 2006; 45:7324.
18. Lauffenburger DA, Horwitz AF. Cell. 1996; 84:359. [PubMed: 8608589]
19. Humphries, MJ. Extracellular Matrix Protocols. Even-Ram, S.; Artym, V., editors. Vol. 522. Humana Press; 2009. p. 203
20. Ogbourne SM, Suhrbier A, Jones B, Cozzi SJ, Boyle GM, Morris M, McAlpine D, Johns J, Scott TM, Sutherland KP, Gardner JM, Le TTT, Lenarczyk A, Aylward JH, Parsons PG. Cancer Res. 2004; 64:2833. [PubMed: 15087400]
21. Kuang Y, Xu B. Angew Chem Int Edit. 2013; 52:6944.

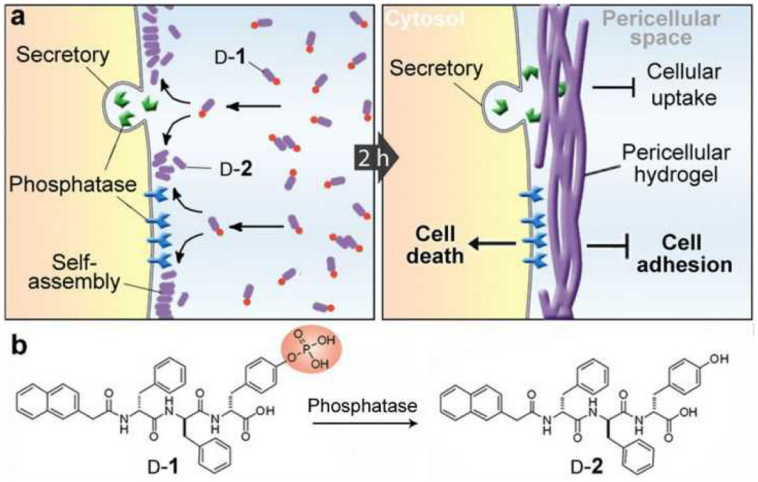

Figure 1.

a) Enzyme catalyzed formation pericellular hydrogel/nanonets to induce cell death. b) Molecular structures of the precursor (D-**1**) and the hydrogelator (D-**2**).

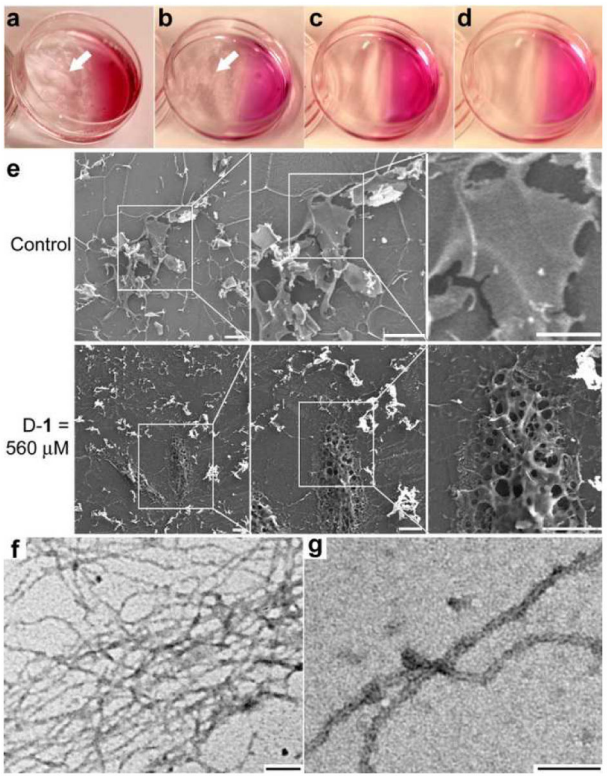

Figure 2.

Enzymatic formation of the hydrogel/nanonets on the cells. Optical images of the HeLa cells incubated with D-**1** at (a) 560, (b) 280, and (c) 140 μM, or with D-**2** at (d) 560 μM for 2 h. White arrows point at the hydrogel/nanonets. e) SEM images of freeze dried HeLa cells treated with D-**1** at 0 μM (control) or 560 μM for 2h. Scale bar = 10 μm. f) Negative stained TEM images of the pericellular hydrogels on the HeLa cells treated by D-**1** at 280 μM. g) High magnification image of the nanofibrils in Fig. 2f. Scale bar in f and g is 100 nm.

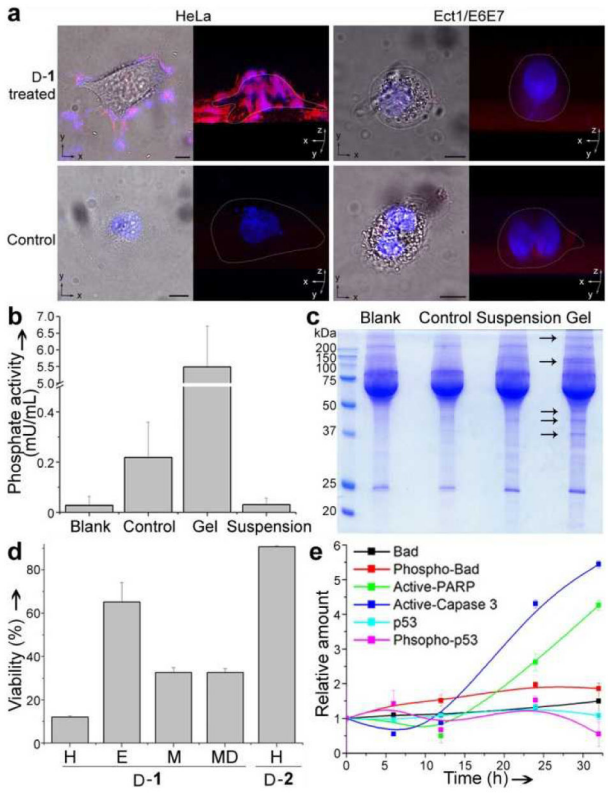

Figure 3.

The pericellular hydrogel/nanonets inhibit cancer cells. a) Overlaid images and 3D stacked z-scan images of Congo red and DAPI stained HeLa and Ect1/E6E7 cell treated by D-**1** or just culture medium as control for 12 h. HeLa cells treated by D-**1** at 280 μM; Ect1/E6E7 cells treated by D-**1** at 560 μM. Scale bar = 10 μm. White dots outline the cells. b) Comparison of phosphate activity in blank medium (Blank), medium incubated with HeLa cells (Control), pericellular hydrogels on HeLa cells treated by D-**1** at 560 μM (Gel), and the suspension medium of HeLa cells treated by D-**1** at 560 μM (Suspension). c) SDS-PAGE showing the protein composition in the Blank, Control, Gel, and Suspension. Arrows point at protein bands that appear only in the lane of the Gel. d) Cell viabilities of HeLa (H), Ect1/E6E7 (E), MES-SA (M) and MES-SA/Dx5 (MD) cells treated by 280 μM of D-**1** or HeLa cells treated by 280 μM of D-**2** for 48 h. e) Change of relative amount of apoptosis signal molecules over time in HeLa cells treated by D-**1** at 280 μM.